ISSN (Online) 2456-1290
International Journal of Engineering Research in Mechanical and Civil Engineering (IJERMCE)
Vol 2, Issue 4, April 2017

Experimental and Computational Analysis of Heat Transfer, Fluid Flow & Pressure Distribution of Multi-Jet Impingement Cooling on Concave Surfaces

[1] Satheesha V, [2] B. K. Muralidhara, [3] C. K. Umesh.
[1] Research Scholar, Bangalore University, Bengaluru and Assistant Professor, RajaRajeswari College of Engineering, Bengaluru, Karnataka, India
[2] Former Professor, University Visvesvaraya College of Engineering & Professor, Nitte Meenakshi Institute of Technology, Bengaluru, Karnataka, India
[3] Professor, University Visvesvaraya College of Engineering, Bengaluru, Karnataka, India,

Abstract: **-- Understanding the fluid path lines using carbon black coating method on target plate in Jet impingement process provides information about the interaction between the jets in the array which plays an important role in the cooling performance. Experimental visualization of flow structure on target plate is observed in collision of wall jets after impingement producing complex flow field. The array of jet consists of three impinging jets at equidistant from the central jet. Jet-to-plate spacing (H) to hydraulic diameter of jet (d) ratio varied from 2 to 4 and jets Reynolds number is varied from 1742 to 3649. Computationally obtained flow structure of interacting jets and effects of varying H/d ratio and Reynolds number on fluid flow, heat transfer and pressure distribution are compared with experimental data. Pressure distribution over the target plate depends on Reynolds number and H/d ratio. Convective heat transfer increases with increase in Reynolds number and decreases with increase in jet to plate spacing (H).**

***Keywords*- Heat Transfer, Impingement Cooling, Nusselt Number, flow visualization, Carbon black method.**

I.INTRODUCTION

Flow visualization is an important technique used to study the behavior of impinging jet. Goldstein et.al [1] investigated the behavior of impinging jets on flat, concave and convex surfaces using a smoke wire visualization technique. It shows the comparison of visualization results of impinging jets on flat, convex and concave surfaces issuing jet from a nozzle of diameter d=72.6 mm with Reynolds number of 6000. When considering the effect of curvature on the flow structures, nozzle-to-surface spacing must also be considered due to its strong influence on the flow structure. Mansoo Choi and Han Seoung Yoo et.al [2] described about the h/d and Reynolds number influence on heat transfer rate. The occurrence of secondary peaks and their locations have been explained from the variations of measured velocity fluctuations of wall jet evolving along the stream wise direction. The phenomenon of secondary peaks is widely studied by many researchers. Gardon and Akfirat [3] explained the secondary peaks is due to the result of the laminar –turbulence transition of the wall jet. Gaunter and Livingood [4] suggested that secondary peak point is the point where the product of turbulent kinetic energy and boundary layer velocity become maximum. Many studies explained that secondary peaks disappear when the target wall were placed outside the potential core region.

Vadiraj V Katti and S V Prabhu [5] studied the heat transfer distribution from a row of impinging jet to a cylindrical concave surface. They considered the ratio of diameter of concave surface to the nozzle diameter as 6 and jet to jet spacing as 4 and z/d jet height to diameter varies from 1, 2, 4 and 6. They observed that heat transfer coefficient due to each jet is nearly repeats from inlet to the closed end and it is observed that stagnation point shifts towards the closed end as z/d increases. Hayder Eren and Nevin celik [6] in their paper nonlinear flow and heat transfer dynamics of slot jet impinging on a slightly curved concave surface, they studied the characteristics slot jet. They developed new correlation for Nusselt number and jet Reynolds number. Geuyoung Yang and Mansoo Choi [7] in their experimental study of slot jet impingement cooling on concave surfaces, they considered Reynolds number between 5920-25500 and h/d from 0.5 to 20, they compared rectangular shaped nozzle and round shaped nozzle and found that for round jet, the shear flow region developed from the edge of the nozzle is expanding due to the mixing flow and ambient air and beyond h/d =6 the effect of entrainment penetrate up to the centre line. Evaluation of internal heat transfer for impingement cooled turbine blades by Chupp et.al. [8] gave an empirical

ISSN (Online) 2456-1290
International Journal of Engineering Research in Mechanical and Civil Engineering (IJERMCE)
Vol 2, Issue 4, April 2017

relation connecting r/d, z/d, h/d and Reynolds number using a wildly accepted correlation. They made a heated surface using thin platinum surface. N. Kayansayan [9] built an experimental test set-up for measurements of flow and heat transfer characteristics of confined slot-air-jet flowing through a semi-circular concave channel. Particular emphasis in his experiments on determining the effect of the channel height and the Reynolds number on the impingement surface pressure and the heat transfer distributions. He plotted the variation in the experimentally measured local Nusselt number distribution with channel height (H) and jet Reynolds number (Re). Neil Zuckerman [10] used numerical models to simulate the heat transfer on a cylindrical target under an array of radial impinging slot jets. V2-f and SST models were selected based on accuracy and computation speed.

From the impingement literature, it has been found less work is done on concave surfaces with low Reynolds number ranges from 1742 to 3649. Mainly in transition region from laminar to turbulent. Experimentation is carried out to study the flow pattern, static pressure distribution and local heat transfer distribution on concave surface with varying the Reynolds number and varying the target plate distance to jet diameter ratio from 2 to 4. Flow visualization on a target plate is done to study the flow pattern characteristics quantitatively. The traces of oil lamp black visualization technique is used to understand the characteristics of fluid flow after jet impingement and used as basic information for studying behavior of impinging jets. The present experimental work is compared with CFD (Computational Fluid Dynamics) results. CFD results for pressure distribution and local heat transfer coefficients have less than 15% error at stagnation point.

2. EXPERIMENTAL DETAILS

The schematic layout of experimental set up is shown in Figure 1.

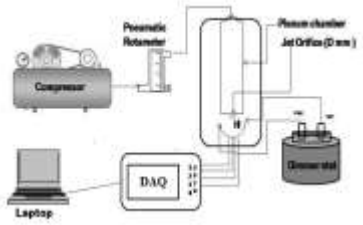

Figure.1 Schematic diagram of experimental set-up

Experimental setup consists of an air supply unit including an air compressor, air tank, filter, pressure regulator, and flow meter, nozzle, and an impingement surface. Cooling jet for the experiment obtained by using different orifice plate geometry at the nozzle exit. The air is supplied by the air compressor which passes through the filter and then goes through a high precision pressure regulator where air pressure is adjusted to the required pressure. The pressurized air is injected into the plenum chamber containing a mesh screen to reduce the flow fluctuations at the nozzle inlet. Finally, the pressurized air goes through the orifice and generates the jet. The flow rates were measured from the Rota meter.

2.1 Flow visualization on the target plate

Flow visualization experiment is conducted with oil-lampblack technique. The target plate is coated with mixture of kerosene and lamp black powder in correct proportions. The lamp black coated target surface is kept beneath target plate for about 60 seconds for impinging. The characteristics of the flow path lines on the plate are captured by camera.

2.2 Measuring pressure distribution on target plate

Pressure distribution on the target plate is measured by using ethyl alcohol in multi-tube manometer. The target plate is drilled and 2 mm diameter plastic tubes were connected as pressure tapings and this intern connected to ethyl alcohol manometer by 2 mm diameter plastic tube.

2.3 Heat transfer measurement

The rate of heat transfer is measured on heated target plate and by impinging cold air jet on it. The target plate is heated by a similar shaped heating plate placed below the target plate. Heating plate is attached to the target plate to heat the entire surface uniformly. AC current is supplied to the dimmer stat which controls the voltage and thus constant heat flux is maintained. The Voltage (V) and Current (A) are tabulated.

In order to keep the bottom surface as adiabatic, two layers of asbestos insulating sheets were used (Thermal conductivity of 0.08 W/m2k). To measure the temperature of the heated surface k-type thermocouples are used. The surface temperature is measured through the thermocouples, which are connected to the data acquisition

ISSN (Online) 2456-1290
International Journal of Engineering Research in Mechanical and Civil Engineering (IJERMCE)
Vol 2, Issue 4, April 2017

system. The steady state temperature are noted while jet impingement on target plate.

2.4. Computational Methodology

The present experiment is simulated computationally in Ansys 14.5. Geometric model is created similar to experimental model. It consists of target plate of 200X200 mm square impingement plate. The distance between the impingement plate and the jet exit is varied to obtain H/d ratio 2, 3 and 4. The spacing between two jets is C= 20 mm.

Ansys Fluent solves Navier stokes equations on each Finite volume element. Figure 2 shows the meshed part of the geometry, it includes tetrahedral geometry and 15 inflation layers to capture the boundary layer effect on the target surface.

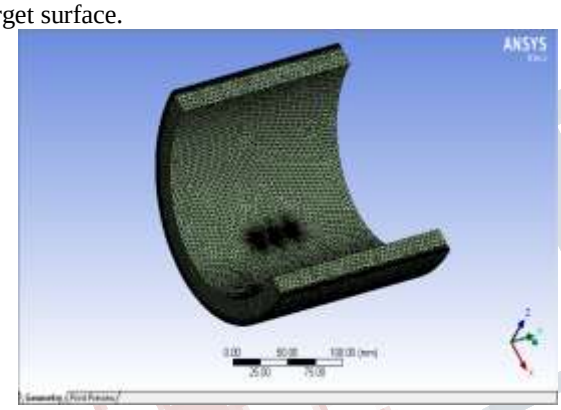

Figure 2: Meshed part of geometry

A Specified mass flow rates at inlet is set at entry to orifice plate. Constant ambient pressure outlet condition is imposed. The flow is assumed to be steady and incompressible, the fluid properties are assumed to be constant. A finite volume based solver is used for solving the governing continuity, momentum and turbulence-model equations.

2.5 Data Reduction

Pressure is calculated by using **$P= \rho*g*H$**

In this case ethyl alcohol manometer is used

The density of the ethyl alcohol (ρ) is 790 kg/m^3

Acceleration due to gravity is (g) is 9.81 m/s^2

Coefficient of pressure is calculated by using

$C_p= (P-P_o)/(0.5*\rho_o*V_o^2)$

P is the stagnation pressure

P_o is atmospheric pressure 101.325 kPa.

ρ_o is density of free stream air 1.225 Kg/m^3

V_o is the velocity of the mass flow

2.6 Calculations to find heat transfer coefficient and Nusselt number

Nusselt Number, Nu = (h*d)/k

The diameter of the jet, d =5mm

Where h is heat transfer coefficient, h = q/(∇T)

Temperature difference, $\nabla T= (T_f-T_i)$

Constant heat flux, q=460 W/m^2

Thermal conductivity of air, k = 0.0242 (W/m.K).

3. RESULTS AND DISCUSSIONS

3.1 CFD results for Pressure distribution at Re 1769 and H/d 2, 3, 4

It can be seen that jet pressure is maximum at the stagnation point and axis-symmetric in nature. The shape of distribution is circular. Since the Reynolds number lies in laminar region, the pressure produced is too low as shown in figure 3.

Pressure contours obtained from the computational analysis shown in the Figures 3. It has been observed that for Re 1769 and H/d ratio of 2 the high pressures is produced at the centre when compared to other jets. As the H/d increases impinged area also increases until the potential core region is present. Pressure contours shows there is more mixing of the flow in the mixing region as H/d increases. The centre jet impinged area increases where the pressure is less compared to the adjacent jets. As the H/d ratio increases the potential core region in jet depletes as the flow reaches the impingement surfaces. The difference in velocity contours is obtained because of the variation in momentum exchange between the fluid jet and ambient.

ISSN (Online) 2456-1290
International Journal of Engineering Research in Mechanical and Civil Engineering (IJERMCE)
Vol 2, Issue 4, April 2017

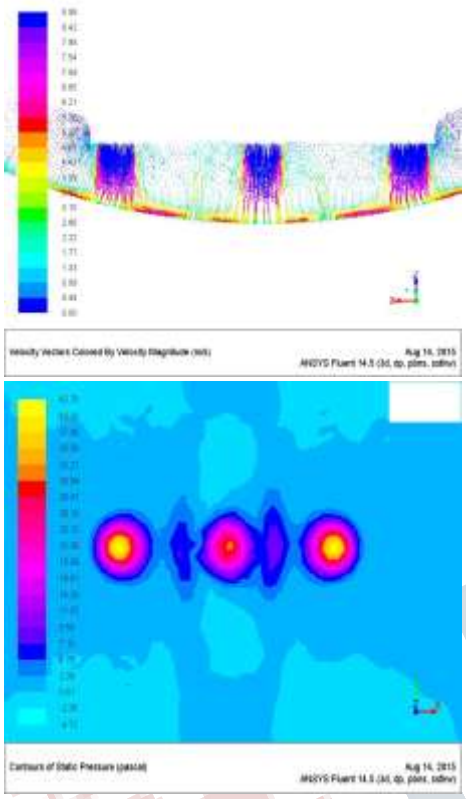

Figure 3. Computed velocity contours and contours of static pressure for H/d=2 and Re=1769.

It can be seen that the region between two jets creates increase in pressure at that point. Since H/d is 2, the potential core will not touch the target plate. But the red circle in the contours shows the increased velocity on the target plate. Jet distributes itself more along the z direction due to easiness in passage which is open to the atmosphere. If the potential core touches the target surface turbulence produced will be more.

Maximum pressure developed at the stagnation point where the jet hits the surface. In all cases mixing of jet is observed, Vortex formation is more in the case of H/d =2 and vortex touches the plenum for H/d=2. It is seen that maximum pressure obtained at H/d=2 due to less space between jet entrance and target plate. In all 3 case it is observed that the potential core will not touch the target plate. The secondary peak of pressure is due to the stagnation produced at the exact point of jet mixing. It is at the centre of two jets. But the secondary peek pressure remains almost same for all H/d.

It is clear that jet height determines the mixing of two jets. As the height increases, the jet lose its velocity due to shearing and atmospheric interaction, thus producing low velocity at impingement region and magnitude of pressure distribution also decreases. In all cases, secondary peek remains same at midpoint of two jets. The vortex formed between the jets touches the surface at H/d=2 and it is due to higher velocity. Zero velocity is found at the center of two jets. This is the point where two jets will interact. It mixes and moves upwards. The point of contact is again comes as stagnation point where the secondary peek is maximum.

It is observed that all the plots for different Reynolds number are similar but only the value of the pressure is different. It confirms that the distribution of the pressure on the concave surface remains same for all the Reynolds number considered. As the H/d ratio increases for a Reynolds number then the peak values tend to move from left side to right side, this pattern is observed in each Reynolds number. As Reynolds number is high, the mixing take place effectively thus creating stagnation region on the mixing point. The height of the jet up wash remains same in H/d =3 and H/d=4.

3.2 Pressure measurement on target plate

The pressure is measured with the help of multi tube manometer in which ethyl alcohol of density 790 Kg/m3 is used.

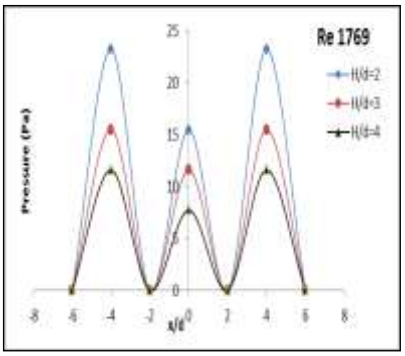

Figure. 4(a). Experimental pressure for H/d=2, 3, 4 and Re=1769

ISSN (Online) 2456-1290
International Journal of Engineering Research in Mechanical and Civil Engineering (IJERMCE)
Vol 2, Issue 4, April 2017

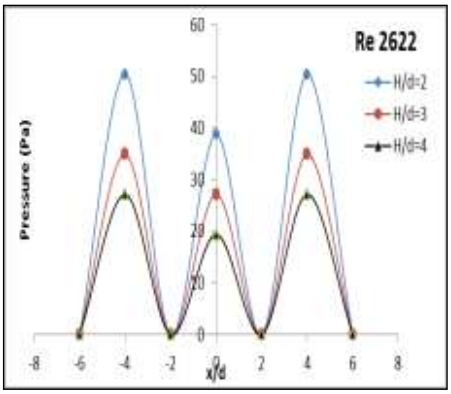

Figure 4(b): Experimental pressure for H/d=2, 3, 4 and Re=2622.

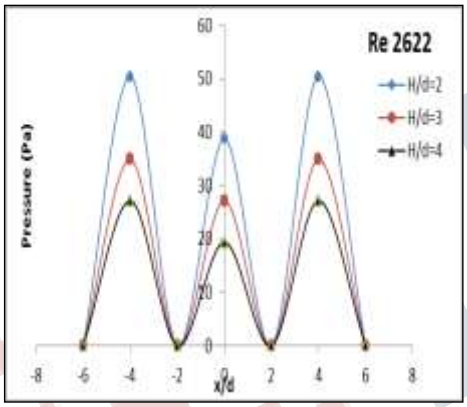

Figure 4(c): Experimental pressure for H/d=2, 3, 4 and Re=3496.

From figure 4.a, figure 4.b and figure 4.c for different H/d ratios it is clear that as the H/d ratio goes on increasing for a Reynolds number the pressure on the concave target plate goes on reducing. As jet impingement is made on the concave surface of the plate from the jets which are drilled in the flat surface, H/d ratio is considered from the centre jet among the three jets. Due to the same reason the distance between the curved surface and the end jets will be less, distance between curved surface and centre jet will be more and hence it is observed that the pressure at the end jet region is high and at the middle jet low pressure is produced. For Re 1769 and H/d=2 pressure of 23.37 Pa is observed at the peak and as the H/d ratio increases to 3 and 4 the pressure reduces to 15 Pa and 11.64 Pa at the peak.

3.3 Visualization of pressure distribution on the target plate:

Visualization is an important technique to see the behavior of the flow quantitatively. Figure 5(a) and 5(b) shows the characteristics of fluid flow on the traces of lamp black on impingement surface. The Computed and experimentally visualized flow structures qualitatively agree well and hence confirms the correctness of the computation.

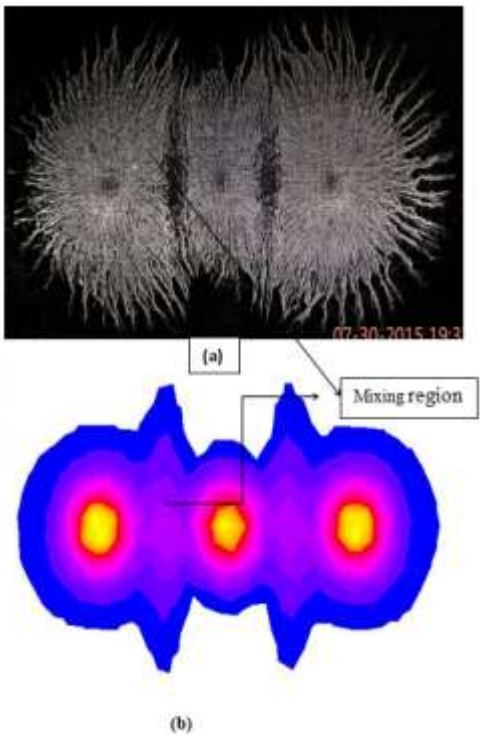

Figure 5. a, b. (a) Experimentally visualized flow structure and (b) Computed pressure contours on target plate.

3.4 Pressure distribution on the target plate at H/d=2

For very low Reynolds number jet impingements flow velocity will be very less. It's difficult to capture the images of those distributions. But for an H/d ratio of 2 and Re=1769 the following pressure distribution has been captured. The distribution of the path lines shows there is no effect of vortex formation and the jets are impinging freely on the target plate.

ISSN (Online) 2456-1290
International Journal of Engineering Research in Mechanical and Civil Engineering (IJERMCE)
Vol 2, Issue 4, April 2017

Figure.6(a) Flow distribution of painted carbon black on concave surface for H/d=2 and for Re=1769

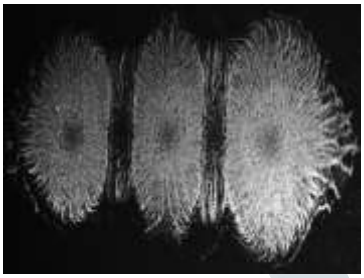

Figure.6(b).Flow distribution of painted carbon black on concave surface for H/d=2 and for Re=2622

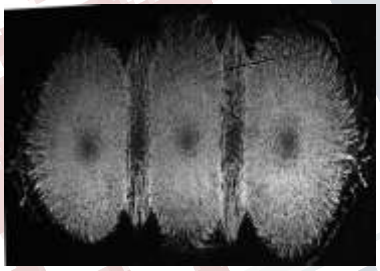

Figure.6 (c).Flow distribution of painted carbon black on concave surface for H/d=2 and for Re=3496.

For a H/d =2 and jet Reynolds number 1769, since the jet velocity is so small the pressure produced on the target surface is small and it is clearly observed that less effects are produced on the target plate in fig 6 (a). The contours obtained from experimental and simulation show similarity in nature. It is clear from the experimental visualization that the mixing region is not effectively produced at low Reynolds number. From figure 6 (b) and 6 (c) it is observed that as the Reynolds number increases the formation of the vortex in between the jets increases and so does the turbulence between the jets.

3.5 Pressure distribution on the target plate at H/d=3

As the H/d ratio increases for a Reynolds number the area of the impinged area goes on reducing this is due to the potential core region of the flow. The length of the potential core region will be constant for a given Reynolds number as explained earlier. As the H/d ratio increases till potential core region the area of impingement increases after that the impinged area tends to decrease.

Figures 7. (a): Flow distribution of painted carbon black on concave surface with H/d=3 and Re=1769.

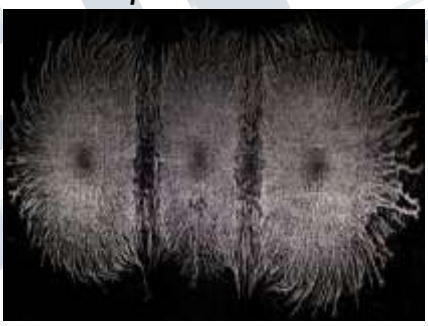

Figures 7. (b): Flow distribution of painted carbon black on concave surface with H/d=3 and Re=2622.

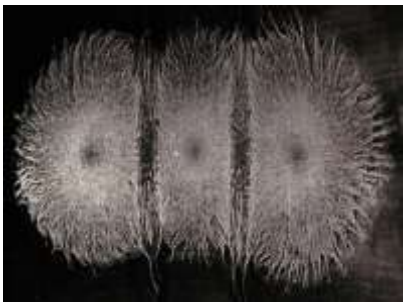

Figures 7. (c): Flow distribution of painted carbon black on concave surface with H/d=3 and Re=3496.

From Figures 7. (a), (b), (c) the distribution of carbon

ISSN (Online) 2456-1290
International Journal of Engineering Research in Mechanical and Civil Engineering (IJERMCE)
Vol 2, Issue 4, April 2017

black on concave surface for H/d=3 for different Reynolds number shows the increase in the stagnation pressure. As the Reynolds number increases from 1769 to 3496 the space between the jets which is called as mixing region it gets smaller and smaller. For Re 3496 Figures 7.(c) the mixing region is very small, it shows that as the Reynolds number increases the mixing region goes on reducing for a same jet spacing due to higher turbulence in the flow.

3.6 Pressure distribution on the target plate at H/d=4

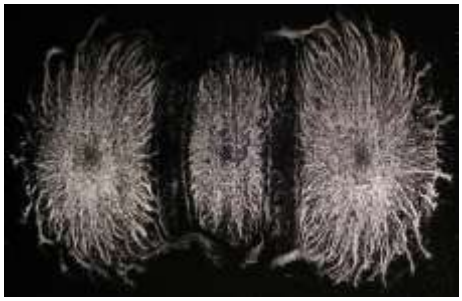

Figures 8 (a). Flow distribution of painted carbon black on concave surface with H/d=4 and Re=1769.

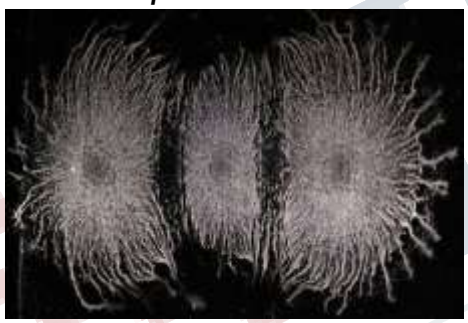

Figures 8(b): Flow distribution of painted carbon black on concave surface with H/d=4 and Re=2622.

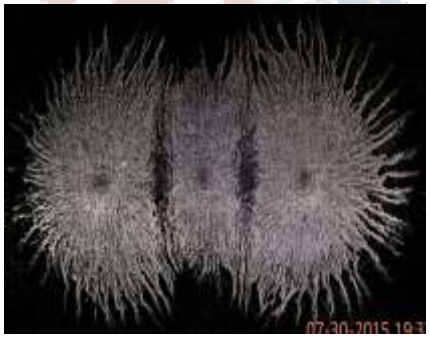

Figures 8(c): Flow distribution of painted carbon black on concave surface with H/d=4 and Re=3496

For H/d=4, increase in Reynolds number will increase the pressure but the area of distribution will decrease due to increase in height. The experiment is repeated for 3 times in every case, no such deviations are observed. Flow distribution of painted carbon black shown in figure 8.(a),(b),(c) clearly shows the wall jets of two adjacent flows collide each other resulting in another local stagnation region or boundary layer separation. This effect provides more heat transfer rate in the stagnation region location.

3.7 Experimental Heat Transfer Analysis

Experiment is conducted with electrically heating of the target plate, which consists of thermocouples. Temperature data is collected through data acquisition system. Initial temperature is measured before impingement and temperature after impingement also measured on all 7 channels spaced 10 mm apart. It is observed that increase in Reynolds number increases the heat transfer coefficient for same H/D ratio. It is also observed that the heat transfer impingement is not axisymmetric in nature. Maximum heat transfer obtained on the first (centre) jet and there is reduction in heat transfer rate for second jet it is situated at x/d= -4, 4.

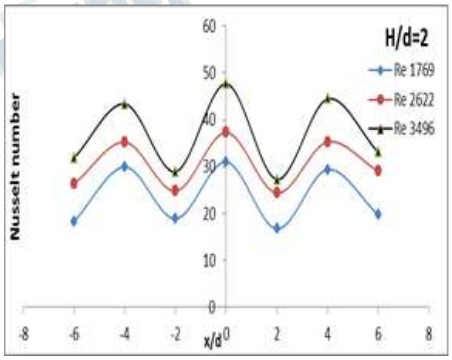

Figure.9 Experimental Nusselt number distribution for H/d=2, Re=1769, 2622, 3496

Highest heat transfer effect is observed at x/d= -4, 0, 4 i.e. directly below the jet. This may considered as localized cooling due to jet. The space in between the jet is also cooled with an averaged heat transfer of 150 W/m2 which means the mixing of two jets effectively transfer the heat. It is clear from the figure 9 that heat transfer increases with

ISSN (Online) 2456-1290
International Journal of Engineering Research in Mechanical and Civil Engineering (IJERMCE)
Vol 2, Issue 4, April 2017

increase in Reynolds number. Maximum local heat transfer is obtained at Re 3496. Its value is about 207.6 W/m2. It is also observed that heat transfer decreases as compared with H/d= 2 because of increase in jet to plate spacing.

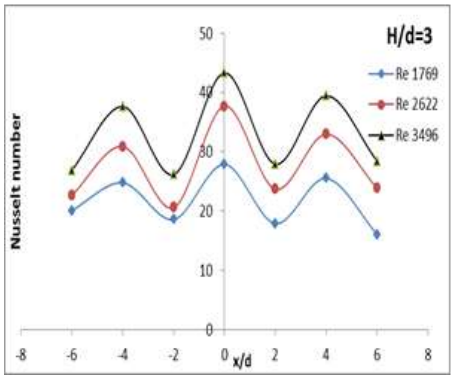

Figure:10. Experimental Nusselt number distribution along x/d ratio for H/d=3 Re=1769, 2622, 3496

From figure.10 the highest heat transfer effect is observed at x/d= -4, 0, 4 i.e. directly below the jet called as stagnation zone. This may considered as localized cooling due to jet. The space in between the jet is also cooled with an averaged heat transfer of 150 W/m2 which means the mixing of two jets effectively transfer the heat.

From the figure 11 that Heat transfer increases with increase in mass flow rate and Reynolds number. Maximum local heat transfer is obtained at Re 3496.Its value is about 172 w/m2. It is also observed that heat transfer decreases as compared with heat transfer results of H/d= 2, H/d=3 because of increase in jet to target spacing.

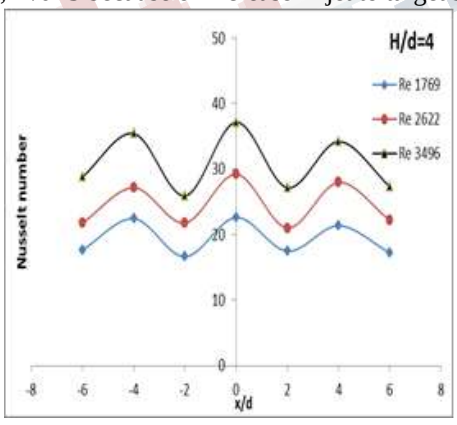

Figure 11: Nusselt number distribution along centerline for H/d=4, Re=1769, 2622, 3496

From fig 11 it is observed that local heat transfer is more for Re 3496 compared to Reynolds number 1769, 2622. It is due to increased velocity and increased turbulent effect. The coefficient of heat transfer and Nusselt number also increased due to mixing of jet. The average heat transfer at this region is 125 W/m2.

3.8 Computational results for Heat transfer analysis

Heat transfer results obtained for H/d= 2

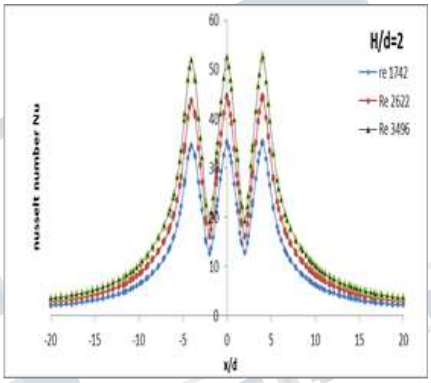

Figure 12:Variation of Nusselt number at H/d = 2 and Re=1769, 2622, 3496

From figure 12 it is clear that Nusselt number increases with increase in Reynolds number. It is also found that centre jet has more Nusselt number as compared to other two jets i.e. Nusselt number for central jet is slightly more than other two jets. This type of observation can be seen in all case of impingement for H/d =2. In CFD results there is no secondary peak observed for heat transfer analysis.

Heat Transfer analysis for H/d=3

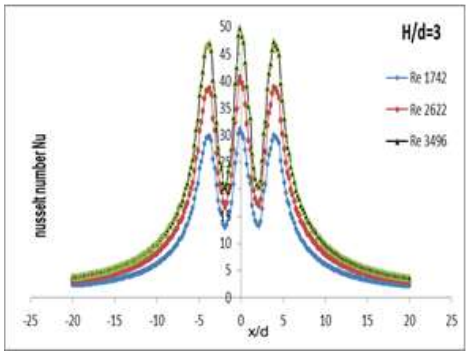

Figure 13 Variation of Nusselt number at H/d = 3 and Re=1769, 2622, 3496

ISSN (Online) 2456-1290
International Journal of Engineering Research in Mechanical and Civil Engineering (IJERMCE)
Vol 2, Issue 4, April 2017

At H/d=3 more Nusselt number is found at Re=3496. Maximum heat transfer is obtained at the stagnation point it is 5-6% more than the other two peaks. This trend is obtained in all Reynolds number. Maximum pressure is produced exactly at the stagnation point but in the case of Nusselt number and heat transfer rate there is slight decreased. This decrease is observed in all case of impingement.

It is observed that Re=3496 has higher heat transfer rate as compared to Re 1769, 2622 because of higher turbulence created for Re=3496 and Nusselt number is higher for higher Reynolds number. It also observed that Nusselt number is decreased for H/d=3 when compared with H/d=2.

Heat Transfer analysis for H/d=4

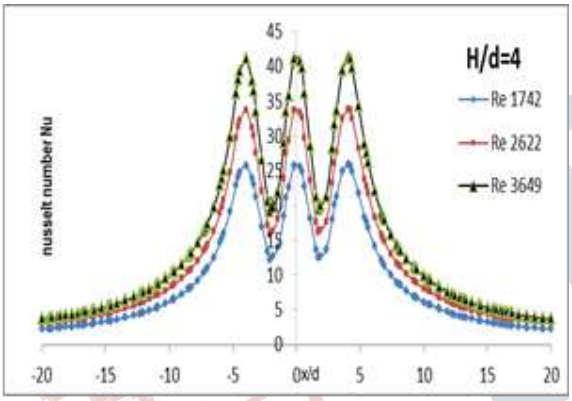

Figure 14. shows the variation of Nusselt number at H/d =4 and Re=1769, 2622, 3496

From figure 14 it is clear that Nusselt number goes on decreasing with increase in H/d ratio due to less turbulence created between two jets. It is observed that Re 3496 produces more heat transfer as compared to Re 1769 and Re 2622 because of larger turbulence created at Re 3496. So Nusselt number is also larger for Re 3496 as compared to Re 1769 and Re 2622. It is also observed that Nusselt number is remains lower for H/d=4 as compared with H/=2 and 3, because of increase in the spacing between jet and target.

4. CONCLUSIONS

An experimental work has been carried out for circular multi jet impingement on a semi-cylindrical curved plate to study the pressure distribution and local heat transfer coefficient at low Reynolds number based on exit condition varied from 1742 to 3649 and jet to target spacing is 2 to 4 times of nozzle diameter. Computational work also performed using Ansys 14.5 software and comparison is made with experimental results. Based on the experimental and computational work following conclusions have been drawn.

- Pressure distribution over the target plate depends on Reynolds number and H/d ratio. As Reynolds number increases pressure distribution also increases for constant H/d ratio.

- At stagnation point Pressure goes on decreases with increase in H/d ratio.

- For all H/d ratio considered the heat transfer increases with increase in Reynolds number at radial locations.

- For all Reynolds numbers considered for study the Nusselt number at the stagnation point decreases with increase in H/D ratio. This may be due to the near wall turbulence intensities and flow acceleration.

- Convective heat transfer increases with increase in Reynolds number and decreases with increase in jet to plate spacing.

- In computational results secondary pressure peaks are observed for H/d =2 and 3 but these are not observed for experimental results.

REFERENCES

[1] A.S.Fleischer, K. Kramer, R.J. Goldstein, Dynamics of the vortex structure of a jet impinging on a convex surface , Experimental Thermal and Fluid Science 24 (2001) 169-175.

[2] Mansoo Choi, Han Seoung Yoo, Geunyoung Yang, Joon Sik Lee, Dong Kee Sohn, Measurements of

impinging jet flow and heat transfer on a semi-circular concave surface, Int J Heat and mass transfer 43(2000) 1811-1822.

[3] Gardon R and Akfart. J. C(1965) The roll of turbulence in determining the heat transfer characteristics of impinging jets Int.J.Heat and Mass transfer 8, 1261-1272.

[4] Gaunter J.W Livingood.JNB and Hrycak.P(1970) Survey of literature on flow characteristics of singe turbulent jet impinging on flat surfaces. NASA TN D-5652 NTIS N70 1896.

[5] V Katti and SV Prabhu Heat transfer enhancement on flat surface with axisymmetric detached ribs by normal impingement of circular jets Int. J of Heat and Fluid Flow 29(2008)1270-1284.

[6] Haydar Eren a, Nevin Celik a, Bulent Yesilata b, Nonlinear flow and Heat transfer dynamics of a slot jet impinging on a slightly curved concave surface, Int. Communications in Heat and Mass Transfer 33(2006) 364-371.

[7] Geunyoung Yang, Mansoo Choi, Joon Sik Lee, An experimental study jet impingement cooling on concave surface: effects of nozzle configuration and curvature, Int. Journal of Heat and Mass Transfer 42(1999) 2199-2209.

[8] Raymond E Chupp and Haeold Helmist Evaluvation of internal heat transfer coefficient for impingement cooled turbine airfoils J.Aircraft Vol 6, No 3 1969.

[9] N.Kayansayan, S.Kucuka, Impingement cooling of a semi-cylindrical concave channel by confined slot-air-jet, Experimental Thermal and Fluid science 25(2001) 383-396.

[10] Neil Zuckerman and Noam Lior, Radial Slot Jet Impingement Flow and Heat Transfer on a Cylindrical Target, Journal of Thermodynamics and Heat Transfer Vol.21, No.3, July-September 2007.